sustainability

MDPI

Article

Laboratory Model Tests of Leachate Drawdown Using Vertical Drainage Wells with Vacuum Pumping in Municipal Solid Waste Landfills with High Leachate Levels

Xiaobing Xu [1], Guangyao Li [2,*], Da Ni [3], Cheng Feng [4] and Sifa Xu [4]

[1] School of Civil Engineering and Architecture, Guangxi University, Nanning 530004, China; xiaobingxu@zjut.edu.cn
[2] Key Laboratory of Urban Security and Disaster Engineering of China Ministry of Education, Beijing University of Technology, Beijing 100124, China
[3] Hangzhou Environmental Group, Hangzhou 310022, China; danizjut@outlook.com
[4] College of Civil Engineering, Zhejiang University of Technology, Hangzhou 310023, China; fwovz@outlook.com (C.F.); xusifa@zjut.edu.cn (S.X.)
* Correspondence: geoguangyao@bjut.edu.cn

Abstract: Municipal solid waste (MSW) landfills in China generally have high leachate mounds, which potentially induce severe geotechnical and environmental issues. In this study, laboratory model tests were carried out to preliminarily investigate the performance of vertical drainage wells accompanied with vacuum pumping (VDW-VP) on leachate drawdown in MSW landfills with high leachate levels. Leachate drawdown tests through VDW-VP under conditions with and without gas injection were performed. Different vacuum pressures (0~−9.5 kPa) were imposed during the tests. Results indicated that the leachate pumping processes for both the two conditions were characterized by a stage of continuous effluent followed by a stage of discontinuous effluent, corresponding to the periods before and after the leachate level in the vertical well dropped to the bottom, respectively. During the stage of continuous effluent, as the vacuum pressure increased, the effluent rate decreased and the leachate level in the vertical well needed a longer time to reach the bottom. During the stage of discontinuous effluent, the leachate level in the MSW gradually approached that in the vertical well. A higher vacuum pressure rendered a larger cumulative leachate pumping volume for the condition with a gas injection, but this was not the case for the condition without a gas injection. In addition, some local pore water pressures were observed to suddenly increase and drop under the condition with the gas injection, attributed to the migration of entrapped gas zones. The increase in vacuum pressure might promote the migration of entrapped gas zones and hence increase the cumulative leachate pumping volume.

Keywords: municipal solid waste; leachate drawdown; (dis)continuous effluent; landfill gas; vertical well; pore pressure

check for updates

Citation: Xu, X.; Li, G.; Ni, D.; Feng, C.; Xu, S. Laboratory Model Tests of Leachate Drawdown Using Vertical Drainage Wells with Vacuum Pumping in Municipal Solid Waste Landfills with High Leachate Levels. *Sustainability* **2022**, *14*, 8101. https://doi.org/10.3390/su14138101

Academic Editors: Yutao Pan, Qiujing Pan and Hui Xu

Received: 9 June 2022
Accepted: 29 June 2022
Published: 2 July 2022

Publisher's Note: MDPI stays neutral with regard to jurisdictional claims in published maps and institutional affiliations.

Copyright: © 2022 by the authors. Licensee MDPI, Basel, Switzerland. This article is an open access article distributed under the terms and conditions of the Creative Commons Attribution (CC BY) license (https://creativecommons.org/licenses/by/4.0/).

1. Introduction

Landfilling is the final disposal option for municipal solid waste (MSW) in developed and developing countries [1,2]. To take China as an example, currently, there are nearly 2000 sanitary landfills in operation and these landfills generally have high leachate mounds, which potentially induce severe geotechnical and environmental issues. On one hand, a high leachate level will cause high water pressure at the upper boundary of the bottom liner system, which promotes the migration of leachate pollutants and ensuing pollution into underground water and soil [3,4]. On the other hand, a high leachate level will increase the pore water pressure of the landfilled MSW, which reduces the shear strength of the MSW and so affects the stability of the landfills [5–8]. In addition, a high leachate level may impede the migration and collection of the landfill gas and induce the occurrence of gas

accumulation in the MSW, further increasing the pore water pressure of the MSW [9–14]. It is worth noting that, for the landfills currently in operation or for those to be expanded in the future, the upcoming MSW in the later stage will further increase the leachate levels, and hence aggravate the risk of the aforementioned geotechnical and environmental issues.

To reduce the leachate levels of sanitary landfills, vertical pumping wells are commonly used for leachate drawdown and drainage. However, their performances vary dramatically as the pumping rate of leachate could be as low as 0 m^3/d~2 m^3/d but up to 50 m^3/d, and previous field measurements demonstrate that the leachate levels commonly decrease insignificantly by using vertical pumping wells [15–18]. Field monitoring based on electrical resistivity tomography (ERT) shows that the accumulation of landfill gas normally occurs in the MSW beneath the leachate levels [17,18]. This causes some local MSW regions to have decreasing saturation degrees and even to be fully filled with entrapped gas. With the drainage of leachate from the landfilled MSW around the vertical wells, the confinement of leachate on the entrapped landfill gas is reduced, and the regions fully filled with landfill gas are further expanded. This occupies or twists the flow channels of leachate, thus resisting the drainage of leachate in the later stage.

Previous large-scale experiments observed that the gas pressure below leachate levels increased and decreased rapidly in cycles, due to the accumulation and dissipation of landfill gas [19]. The accumulation of landfill gas was due to the gas generation and the impediment of gas migration caused by leachate. After the gas pressure reached a "breakthrough value", the entrapped gas started to break through the leachate around it and dissipate, leading to a sharp drop in gas pressure. The accumulation-dissipation process of landfill gas reoccurred in cycles with continuous gas generation. A similar phenomenon was observed in the isotropic consolidation test on peat soil with trapped gas bubbles [20].

Vertical wells usually have large influence depths. Vacuum pressure has been applied to vertical wells to achieve a rapid consolidation of soil in soil improvement projects [21–24]. The application of vacuum pressure generates negative pore pressures along the soil surface and along the length of a vertical well. This increases the excess pore pressure gradients, thereby accelerating the discharge of water from soil and thus the consolidation of soil. Inspired by this mechanism, if vacuum pressure is applied in vertical wells that are installed in landfills, the breakthrough pressure of entrapped gas below the leachate levels would be expected to decline, which would accelerate the gas dissipation and migration. On this account, the application of vacuum pressure will eventually contribute to reducing the volume of entrapped gas zones, improving the collection efficiency of landfill gas and mitigating the resistance of landfill gas to leachate drainage. However, limited data have been reported in the literature regarding the application of vacuum pressure in landfills [25]. On the other hand, due to the differences of material composition and water/gas distributions between soil and MSW [26–29], the water flow processes and water/gas interactions in soil and MSW may behave differently. The dewatering performance of vertical wells with vacuum pressure for landfills remains elusive.

In this study, laboratory model tests were carried out to preliminarily explore the performance of leachate drawdown for MSW landfills by using vertical drainage wells accompanied with vacuum pumping (VDW-VP). Sand was used in the model tests to mimic the MSW located deep in landfills. Gas was injected into the sand to simulate the generation and accumulation of landfill gas. The model tests were conducted under the conditions with and without gas injection. Vacuum pressures in the range of 0~−9.5 kPa were imposed for both the two conditions. The hydraulic conditions (including the water level and pore water pressure) of the vertical well and sand and the pumping rate and cumulative pumping volume of leachate were recorded during the entirety of the tests. The observations obtained from the two conditions with and without gas injection were compared and analyzed. The influence of applying vacuum pressure on the performance of leachate drawdown by using vertical drainage wells was revealed. The results of this study

can provide essential data for the understanding of the coupling behavior between the flow of leachate and the migration of entrapped gas in MSW landfills with high leachate levels.

2. Materials and Methods

2.1. Material

Sand was used in the model tests to mimic MSW located deep in landfills. The particle size distribution of the selected sand was similar to a borehole sample of deep MSW in a landfill [30], as shown in Figure 1. Table 1 compares the geotechnical properties and gas production potential (i.e., gas production rate per unit volume of the material) of the sand and borehole sample. It can be seen that the sand had a higher gas production potential (simulated by gas injection) and lower saturated permeabilities to water and gas as compared to the borehole MSW sample. This was favorable for the formation of entrapped gas zones below the leachate level and the evolution of entrapped gas zones in response to the leachate drainage and vacuum pumping. For this reason, using sand to mimic deep MSW is considered to be feasible for a preliminary study.

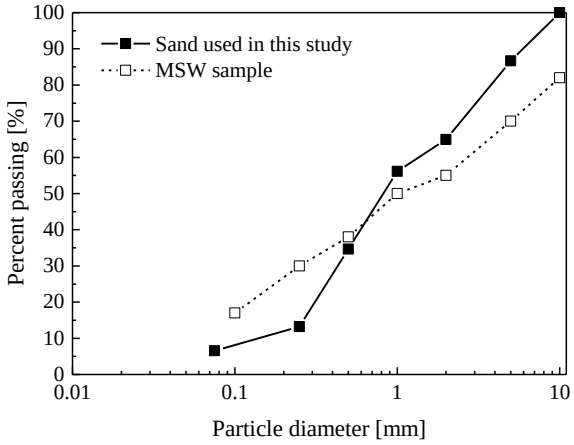


Figure 1. Particle size distribution of the sand in model test. The MSW sample data are from [30].

Table 1. Comparison between the geotechnical properties and gas production potential of the sand and deep borehole MSW sample.

Source	Specific Gravity [–]	Dry Density [Mg/m^3]	Void Ratio [–]	Characteristic Particle Size, d_{10} [mm]	Permeability to Water [m^2]	Permeability to Gas [m^2]	Gas Production Potential [mol/m^3/s]
Sand	2.67	1.653	0.60	0.14	7.20×10^{-13}	1.06×10^{-12}	2.385×10^{-3}
Deep MSW	[a] 2.10	[a] 0.810	[a] 1.56	[a] 0.10	[a] 4.47×10^{-12}	[a] 2.43×10^{-11}	[b] 4.866×10^{-7}~ 4.866×10^{-6}

[a] from [30] [b] from [31].

2.2. Experimental Setup

A model test system was constructed to reveal the process of leachate drawdown using VDW-VP. This system was composed of an experimental box, a water drainage system, a water injection system, a gas injection system, and a vacuum pumping system. The experimental box, made of 5 mm thick steel plates, was 1.6 m in length, 1.0 m in width, and 1.1 m in height (see Figure 2). The schematic profile and schematic sections of the model test system are shown in Figures 3 and 4, respectively. The water drainage system consisted of a vertical well, a peristaltic pump, a water collection bucket, and silicone hoses. The vertical well was simulated by using a PVC pipe (0.8 m in length, 75 mm in outer diameter, and 72.7 mm in inner diameter). The PVC pipe was placed vertically against the middle of a long sidewall of the experimental box (see Figures 3 and 4). The bottom of the

PVC pipe was sealed. The half of the PVC pipe facing the center of the experimental box was perforated within 50 cm from the bottom for the passage of water. The holes punched on the PVC pipe were at vertical and radial spacings of 50 mm and 30°, respectively. The perforated area was wrapped outside with two layers of non-woven geotextiles to prevent soil particles from clogging the holes. A silicone hose (12.9 mm in outer diameter and 10.4 mm in inner diameter) was placed in the PVC pipe for water drainage. One end of the silicone hose extended to the bottom of the PVC pipe and the other end was connected with the peristaltic pump, which provided power for water drainage.

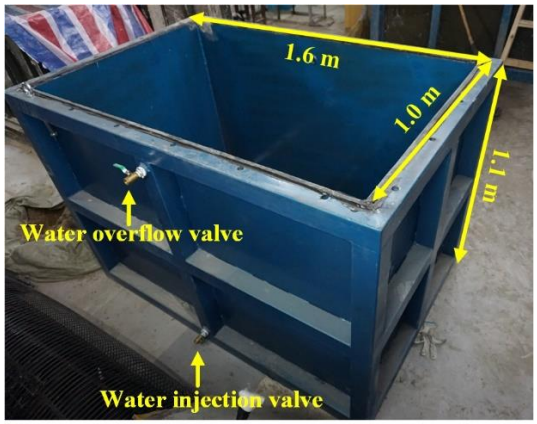


Figure 2. Experimental box.

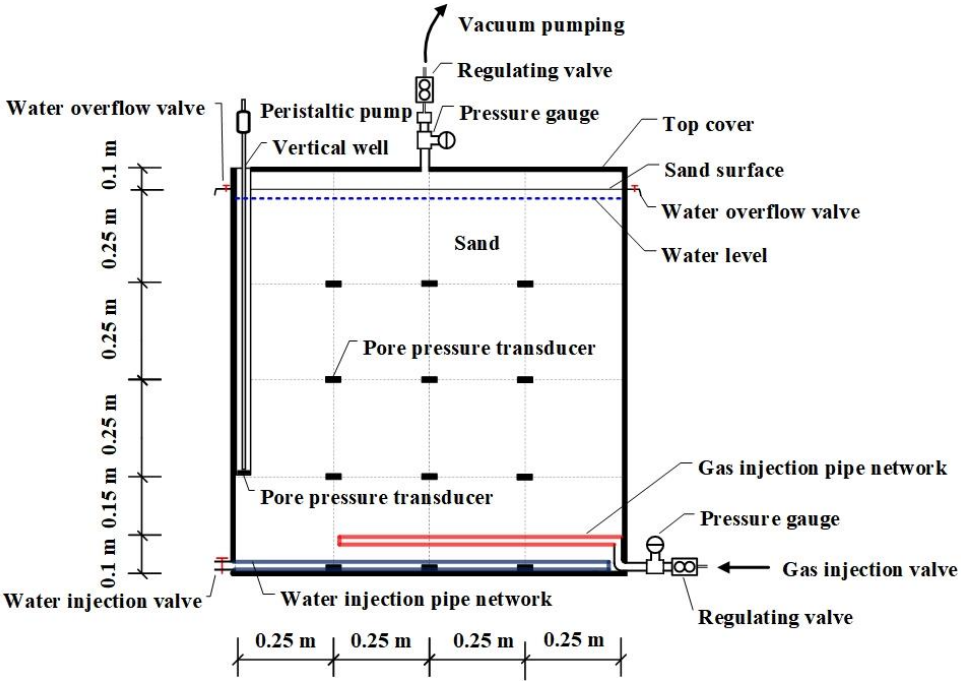


Figure 3. Schematic profile of the model test system. The red lines denote the gas injection pipe network.

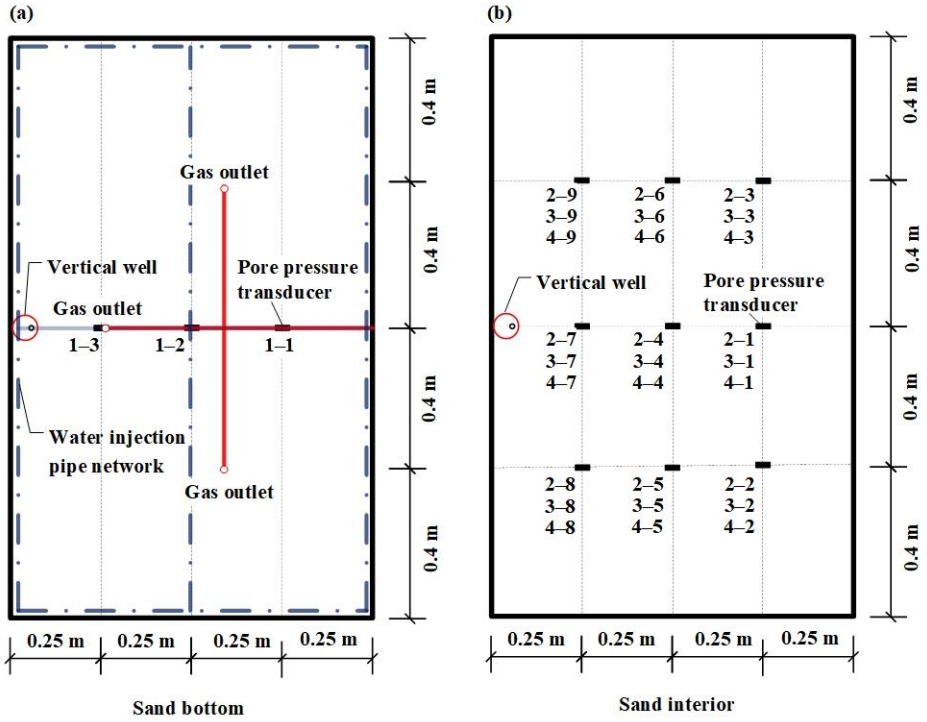


Figure 4. Schematic sections of the (**a**) bottom and (**b**) interior of the model test system. The red lines denote the gas injection pipe network. The red circles indicate the position of the vertical well.

As shown in Figure 5, the water injection system was composed of a water storage bucket, a rectangular water injection pipe network, a water injection valve, and two water overflow valves. The water injection pipe network was horizontally placed at the bottom of the sand. The gas injection system contained a blowing/suction fan, a cross-shaped gas injection pipe network, a gas injection valve, a regulating valve, a gas flowmeter, and a pressure gauge, as shown in Figure 6. The gas injection pipe network was horizontally placed at the bottom of the sand but above the water injection pipe network. The pipes used in both the water and gas injection networks were made of PPR (22 mm in outer diameter and 20 mm in inner diameter) and perforated. The lengths of these pipes are illustrated in Figures 5 and 6. The outsides of these pipes were wrapped with two layers of non-woven geotextiles. As shown in Figure 7, the vacuum pumping system was placed on the top of the experimental box. It was composed of a blowing/suction fan, a gas extraction valve, a regulating valve, and a pressure gauge.

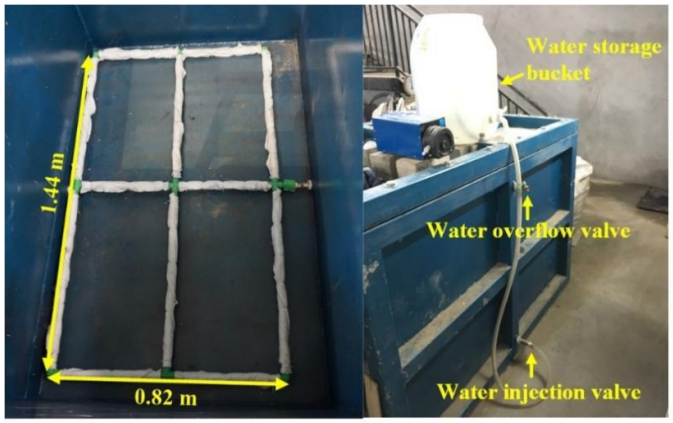


Figure 5. Water injection system.

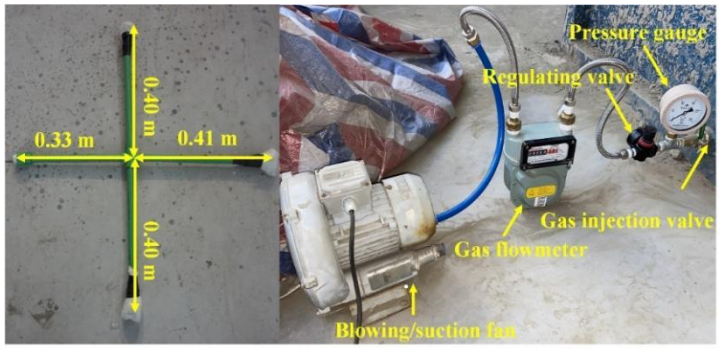


Figure 6. Gas injection system.

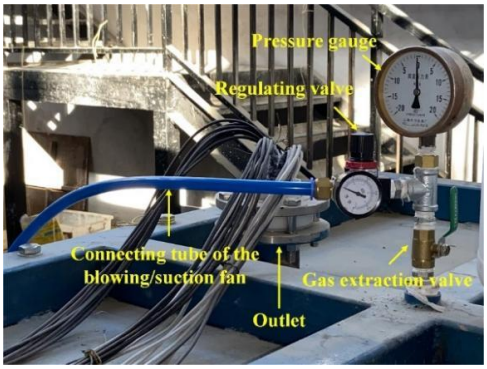


Figure 7. Vacuum pumping system.

During the tests, the ambient temperature, water level, pore pressure, water pumping rate/volume, and gas injection rate/volume were measured. Four nests of pore pressure transducers (DMKY, Nanjing Danmo Electronic Technology Co., Ltd., Nanjing, China) with a measuring range of 0 kPa~100 kPa were installed to measure the pore pressures of the sand, including the upper, middle, lower, and bottom sections as shown in Figure 3. The bottom section had three pore pressure transducers (No. 1-1~1-3). The upper, middle, and lower sections had nine pore pressure transducers in each section (No. 2-1~2-9, 3-1~3-9, and 4-1~4-9). Figure 8 shows the view after the installation of the pore pressure transducers in the middle section. In addition, a pore pressure transducer was arranged at the bottom of the vertical well. Finally, a total of 31 pore pressure transducers were included in the model test system.

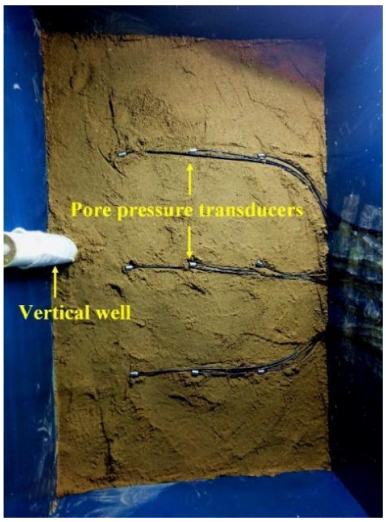


Figure 8. Installation of the pore pressure transducers in the middle section.

2.3. Experimental Operations

After the filling of the sand and the installations of the water drainage system, water/gas injection networks, and pore pressure transducers, the experimental box was covered by the top cover, and the wires of the pore pressure transducers were passed through the outlet of the top cover (see Figure 6). Then, the box and top cover were tightened with bolts. The wires of the pore pressure transducers were finally connected to multi-channel data acquisition equipment. After the connection, the outlet of the top cover was sealed. The initial pore pressures obtained from the multi-channel data acquisition equipment prior to the experiments were recorded. Water was injected into the experimental box through the water injection network. The water injection continued until the water level in the sand exceeded the elevation of the two overflow valves (i.e., 0.95 m high from the bottom of the sand). After that, the overflow valves were closed. Vacuum pressure in the experimental box was then imposed by turning on the blowing/suction fan. A vacuum pressure of −9.5 kPa was maintained for 24 h to evacuate the gas for the saturation of the sand. After the sand was saturated, all the valves were closed and the leachate drawdown test was subsequently initiated.

Table 2 shows the experimental programs, including two groups that corresponded to the two conditions without and with gas injection into the sand. Six different vacuum pressures of 0, −2, −4, −6, −8, and −9.5 kPa were applied for each condition. For group 1 (the condition without gas injection), the target vacuum pressure was first imposed for each case (i.e., 1-a~1-f). Then, the leachate drawdown process was carried out by turning on the peristaltic pump, during which the pore pressures at the bottom of the vertical well and at different depths of the sand were measured. For group 2 (the condition with gas injection), before applying vacuum pressure, a gas injection process was first applied for 5 min, during which the gas injection rate, volume, pressure, and ambient temperature were recorded. Table 3 summarizes the ambient temperature, gas injection pressure, and rate during the gas injection process for each case. The gas injection pressure remained at a constant of 11.5 kPa. The average gas injection rate was 5 L/min, corresponding to a gas production rate of 2.385×10^{-3} mol/m^3/s. After the gas injection ceased, the experimental box was placed without any operations applied for 60 min, to make the sand reach the hydrological equilibrium. Next, the target vacuum pressure was imposed (2-a~2-f). After that, the leachate drawdown test was conducted, during which the following data were recorded: water pumping volume and pore pressures at the bottom of the vertical well and at different depths of the sand. For all the cases in group 1 and group 2, the pumping rates provided by the peristaltic pump were 2.8 L/min and the pumping processes were ceased when the cumulative water pumping volumes reached 141.43 L.

Table 2. Experimental programs.

Group	Case	Gas Injection	Temperature [°C]	Vacuum Pressure [kPa]
1	1-a	Not applied	22	0
	1-b		22.5	−2
	1-c		23	−4
	1-d		23	−6
	1-e		22	−8
	1-f		22	−9.5
2	2-a	Applied	22	0
	2-b		24.5	−2
	2-c		24.5	−4
	2-d		24	−6
	2-e		23	−8
	2-f		22	−9.5

Table 3. Gas injection information for group 2.

Case	Injection Duration [min]	Injection Pressure [kPa]	Injection Rate [L/min]
2-a	5	11.5	4.1
2-b	5	11.5	3.86
2-c	5	11.5	5.12
2-d	5	11.5	5.46
2-e	5	11.5	4.58
2-f	5	11.5	5.44

The state when the sand was completely saturated was taken as the initial state of the mass and volume conservation analyses. Based on the principle of mass conservation of water, there is:

$$m_{w0} - m_{we} = m_{wu} + m_{wl} + m_{wc} \quad (1)$$

where m_{w0} (kg) is the initial mass of the water for the saturated sand; m_{we} (kg) is the mass of the water drained out; m_{wu} is the mass of water in the sand above the water level; m_{wl} (kg) is the mass of water in the sand beneath the water level; and m_{wc} (kg) is the mass of the water in the cavity above the surface of the sand.

During the gas injection stage before vacuum pumping, as the values of m_{we} and m_{wu} are zero, there are:

$$m_{wl} = m_{w0} - m_{wc} \quad (2)$$

$$m_{wc} = \rho_w h_c S \quad (3)$$

where ρ_w (kg/m^3) is the density of water; h_c (m) is the height of water above the surface of sand; and S (m^2) is the area of sand.

During the water pumping stage and after the drainage of the water above the surface of the sand, as the value of m_{wc} is zero, there is:

$$m_{wl} = m_{w0} - m_{we} - m_{wu} \quad (4)$$

The value for m_{we} in Equation (4) can be estimated from the field capacity tests on sand under different vacuum pressures. Therefore, based on the measured m_{w0}, m_{wc}, m_{we}, and m_{wu}, the volumes of water and gas in the sand beneath the water level can be estimated by:

$$V_{wl} = \frac{m_{wl}}{\rho_w} \quad (5)$$

$$V_{gl} = nV_l - V_{wl} \quad (6)$$

$$V_l = h_l S \quad (7)$$

where V_{wl} and V_{gl} (m^3) are the volumes of water and gas beneath the water level; n is the porosity of sand; V_l (m^3) is the volume of sand beneath the water level; and h_l is the height of water level above the bottom of the sand.

It should be noted that, for the above derivation, the height of the sand was assumed to remain unchanged throughout the entirety of the tests. During the water pumping processes, the water levels were funnel-shaped and could be estimated according to the monitoring results of the pore pressures in the sand.

3. Model Test Results

Figure 9 shows the developments of the water levels (the bottom of the sand was defined as the datum) in the sand with time for group 1. The water levels were determined according to the measured pore water pressures at the bottom of the sand. Each data point in Figure 9 was the mean of the three measured values. It can be seen that the water level in the sand for each case decreased monotonically with a reducing rate in response to the increase in time. This implied that the water drainage rate decreased gradually with time.

At the end of the tests, the water levels of all the cases approached 0.25 m~0.30 m, close to the elevation of the bottom of the vertical well. Figure 10 shows the developments of the water levels (the bottom of the sand was defined as the datum) in the vertical well with time for group 1. The water level in the vertical well for each case presented a clear two-stage variation with time. During the first stage, the water level decreased linearly with time and the water effluent was observed to be continuous. This was attributed to the sufficient supply of water from the sand to the vertical well. At 29 min~65 min, the water level in the vertical well decreased to 0.25 m~0.30 m and stopped from further decreasing, indicating that the water level had almost reached the bottom of vertical well. Meanwhile, the higher the vacuum pressure, the longer time required to empty the water in the vertical well. After 29 min~65 min, the water level in the vertical well stabilized at around 0.25 m~0.30 m. Note that the water level in the vertical well was still lower than that in the sand. Therefore, the water in the sand would continue to flow into the vertical well. However, the water effluent during this period was observed to be discontinuous, which was due to the insufficient supply of water from the sand to the vertical well. In addition, Figures 9 and 10 indicated that the test ceased at an earlier time for higher vacuum pressure except for the case with the vacuum pressure of 0 kPa.

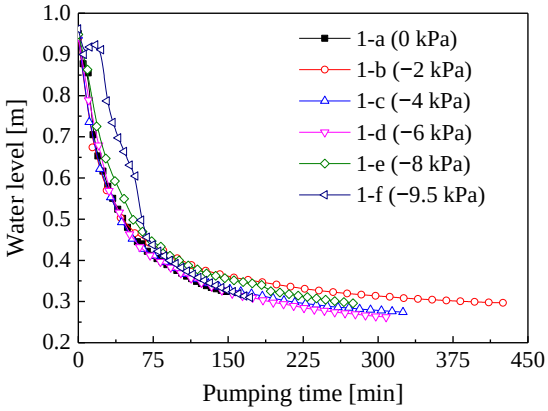


Figure 9. Variations of the water levels in the sand with time for group 1.

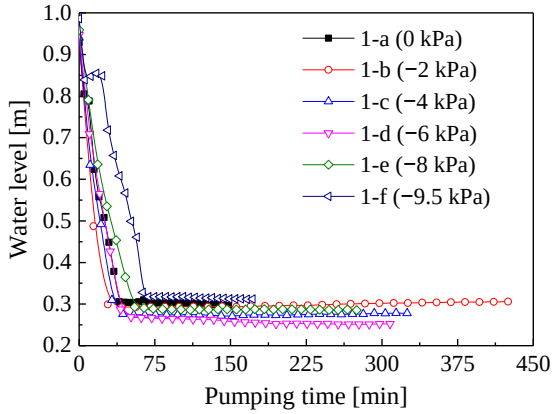


Figure 10. Variations of the water levels in the vertical well with time for group 1.

Figures 11 and 12 show the developments of water pumping rates and cumulative water pumping volumes with time for group 1, respectively. Overall, the water pumping rates decreased gradually with time for all the cases. Before the water level of the vertical well dropped to the bottom (i.e., t < 29 min~65 min), a larger vacuum pressure induced a smaller water pumping rate and a smaller cumulative water pumping volume at given time. This is consistent with the above finding that it took a longer time to empty the water in the vertical well for a higher vacuum pressure. This was because the higher vacuum pressure

in the experimental box reduced the hydraulic gradient applied on the pumping system since the pressure at the outlet of the pumping system was constant. After all the water in the vertical well was pumped out (i.e., t > 29 min~65 min), a higher vacuum pressure could result in a larger water pumping rate and a cumulative water pumping volume at a given time (e.g., t = 65 min~150 min) except for the case with the vacuum pressure of 0 kPa. This indicated that a higher vacuum pressure accelerated the water migration through the sand due to the higher hydraulic gradient in the sand. The higher water pumping rate in this period also resulted in a faster completion of the target water pumping volume for a higher vacuum pressure.

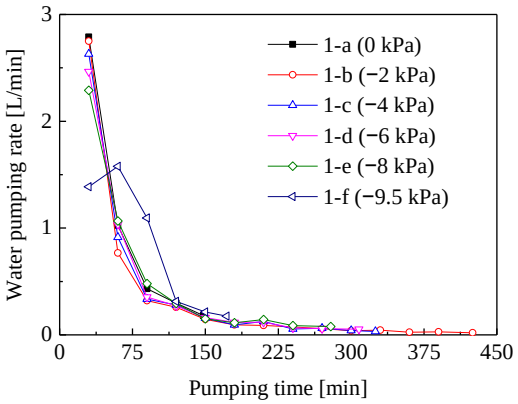


Figure 11. Variations of the water pumping rates with time for group 1.

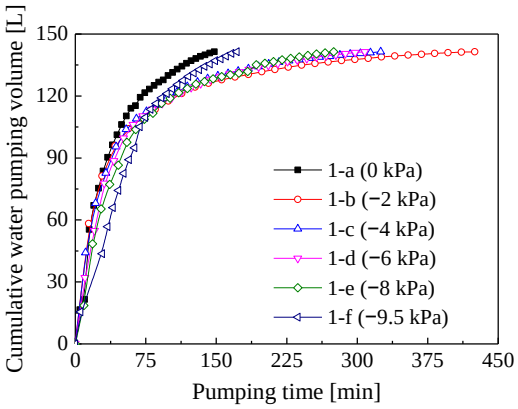


Figure 12. Variations of the cumulative water pumping volumes with time for group 1.

Table 4 shows the information regarding the gas injection and gas accumulation estimated from the measured mass of gas injected and collected before the water pumping for group 2. Table 4 indicated that the pressure of the entrapped gas below the water levels was 1.35~4.26 times the atmospheric pressure. It should be noticed that the volume and mass of the entrapped gas below the water level for each case was relatively close (except for the case of 2-b). This also verified the repeatability of the test to some extent.

Table 4. Information regarding the gas injection and gas accumulation below the water levels for group 2.

Case	Volume of Injected Gas [m^3]	Mass of Injected Gas [kg]	Volume of Entrapped Gas [m^3]	Pressure of Entrapped Gas [Pa]	Mass of Entrapped Gas [kg]
2-a	2.05×10^{-2}	2.73×10^{-2}	6.49×10^{-3}	1.35×10^{5}	1.04×10^{-2}
2-b	1.93×10^{-2}	2.55×10^{-2}	6.83×10^{-4}	4.26×10^{5}	3.41×10^{-3}
2-c	2.56×10^{-2}	3.38×10^{-2}	5.12×10^{-3}	1.44×10^{5}	8.67×10^{-3}
2-d	2.73×10^{-2}	3.61×10^{-2}	6.83×10^{-3}	1.33×10^{5}	1.07×10^{-2}
2-e	2.29×10^{-2}	3.04×10^{-2}	2.05×10^{-3}	2.09×10^{5}	5.04×10^{-3}
2-f	2.72×10^{-2}	3.62×10^{-2}	5.47×10^{-3}	1.41×10^{5}	9.13×10^{-3}

Figure 13 shows the variations of the pore pressures at the bottom of the vertical well and the bottom section of the sand (No. 1-1~1-3) with time for group 2. The horizontal distances between the pore pressure transducers in the sand and the center of the vertical well (denoted by the symbol "D") are also given in Figure 13. For each case, the water effluent was changed from continuous effluent to discontinuous effluent when the water level in the well dropped to the bottom, which occurred at 35 min~64 min. With the increase of vacuum pressure, the time for the water level in the well to drop to the bottom was longer. This was in agreement with those observed in group 1. Additionally, the water level (or the pore pressure) in the sand decreased with a reducing rate with time and finally approached the water level (or the pore pressure) in the vertical well.

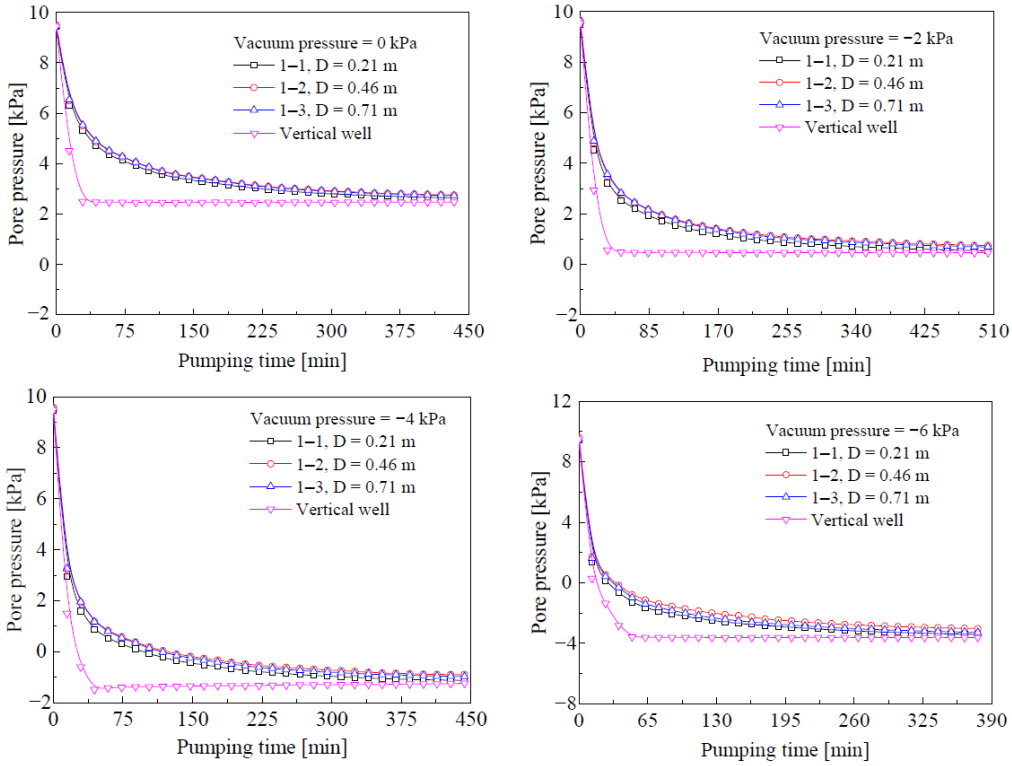


Figure 13. *Cont.*

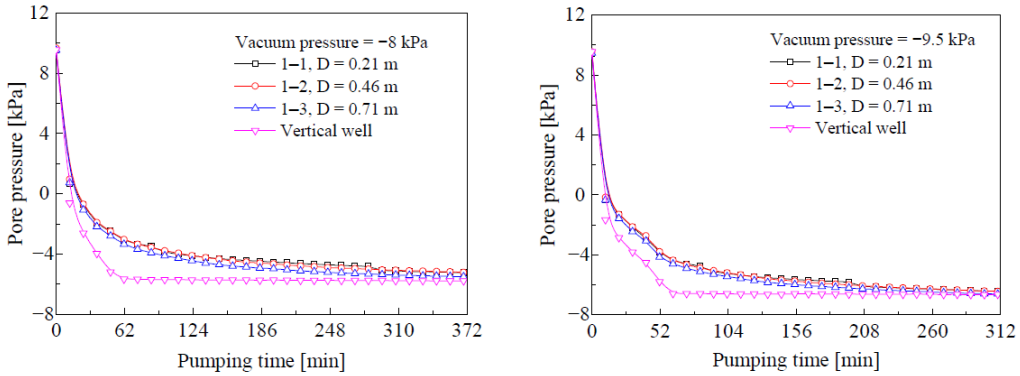


Figure 13. Monitoring results from the pore pressure transducers at the bottom of the well and the bottom section of the sand for group 2.

Figure 14 shows the variations of pore pressures at the lower section of the sand (No. 2-1~2-9) with time under the three different vacuum pressures of 0 kPa (2-a), −4 kPa (2-c), and −6 kPa (2-d). It was observed that some pore pressure transducers at the same distance from the vertical well could give different pore pressures, such as 2-5 and 2-6 under the three vacuum pressures. This was attributed to the non-uniformly distributed entrapped gas zones beneath the water level. Furthermore, the pore pressure measured by the 2-1 pore pressure transducer presented a sudden increase at 200 min in the 2-a case. Similar sudden increases of pore pressures were also recorded by the 2-6 pore pressure transducer at 375 min in the 2-c case and the 2-5 pore pressure transducer at 130 min in the 2-d case. These suddenly increased pore pressures were observed to fall back in later stages. The sudden increase of pore pressure may be due to the movement of entrapped gas to the position around the pore pressure transducer. Subsequently, the flow away of the entrapped gas induced the drop of the pore pressure.

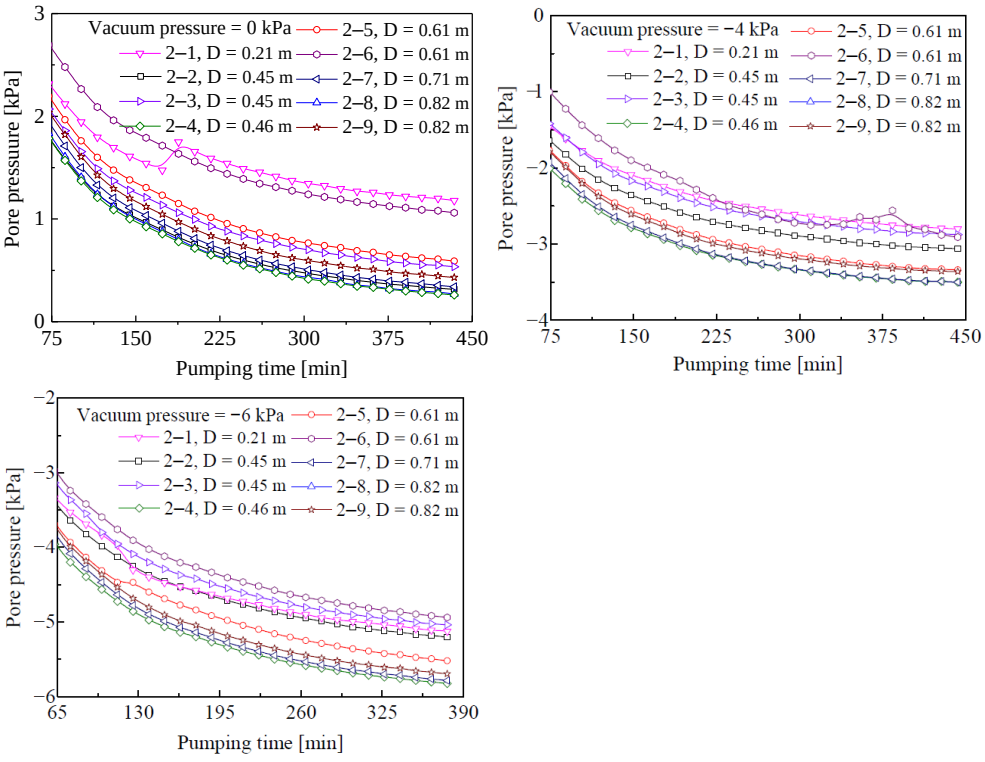


Figure 14. Monitoring results from the pore pressure transducers at the lower section of the sand under three different vacuum pressures.

Figures 15 and 16 show the developments of water pumping rates and cumulative water pumping volumes with time for group 2, respectively. In the stage of continuous effluent, the water pumping rate decreased with the increase of vacuum pressure, while, in the stage of discontinuous effluent, the water pumping rate increased with the increase of vacuum pressure. Note that a higher vacuum pressure led to a larger cumulative water pumping volume in this stage, which was different from that observed in group 1, wherein the case with 0 kPa vacuum pressure produced the maximum cumulative water pumping volume. As the existence of entrapped gas zones in the sand below the water level hindered the water migration from the sand into the vertical well, the above findings, to some extent, indicated that the increase of vacuum pressure contributed to accelerating the breakthrough and dissipation of the entrapped gas zones, thus improving the water pumping capacity. However, due to the limitations of the model size and volume of the entrapped gas zones, the observations of this study were preliminary. The complex coupling behaviors and mechanisms between the flows of leachate and entrapped gas during the leachate drawdown process using VDW-VP remain to be further investigated.

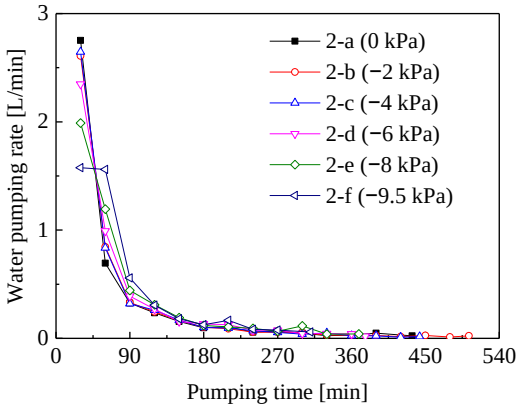


Figure 15. Variations of the water pumping rates with time for group 2.

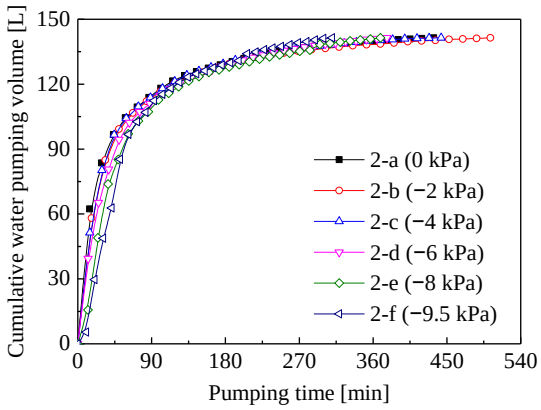


Figure 16. Variations of the cumulative water pumping volumes with time for group 2.

4. Practical Implications of the Study

By performing a series of preliminary laboratory model tests, this study revealed the effect of vacuum pressure on the performance of a vertical well in leachate drawdown for landfills. Under the condition with gas injection, the application of vacuum pressure slows down the discharge of leachate in the vertical well at the early stage (the leachate level needs a longer time to reach the well bottom), but it can obviously accelerate the movement of leachate from MSW to the vertical well at the later stage. Based on the main findings of this study, a VDW-VP structure is proposed to achieve a rapid drawdown of leachate for landfills with high leachate levels, as shown in Figure 17. A well made of galvanized

steel pipe is installed vertically in the MSW, and it is wrapped by a composite drainage net layer, a gravel layer, and a geogrid layer from inside to outside. The well pipe is divided into three segments from top to bottom. The upper segment is not perforated for sealing the vacuum pressure. The middle segment is perforated for the passage of leachate/gas. The lower segment is not perforated with the bottom blocked. One leachate flow pipe is placed in the well with its end connected with a submersible pump, which is located at the bottom of the well pipe. One pore pressure transducer is also placed in the well and the elevation of its location must be higher than that of the submersible pump. The top of the well pipe is provided with a vent connected to a gas extraction pump, which extracts gas to generate a vacuum pressure in the well pipe. At the beginning of leachate pumping, the leachate level in the well is high. In this case, the vacuum pressure is not applied to achieve faster drainage of leachate in the well, according to the findings of this study. When the pore pressure at the monitoring position in the well decreases to zero, it indicates that the leachate level has dropped to the well bottom. At this moment, vacuum pressure is applied to accelerate the movement of leachate from the MSW to the well.

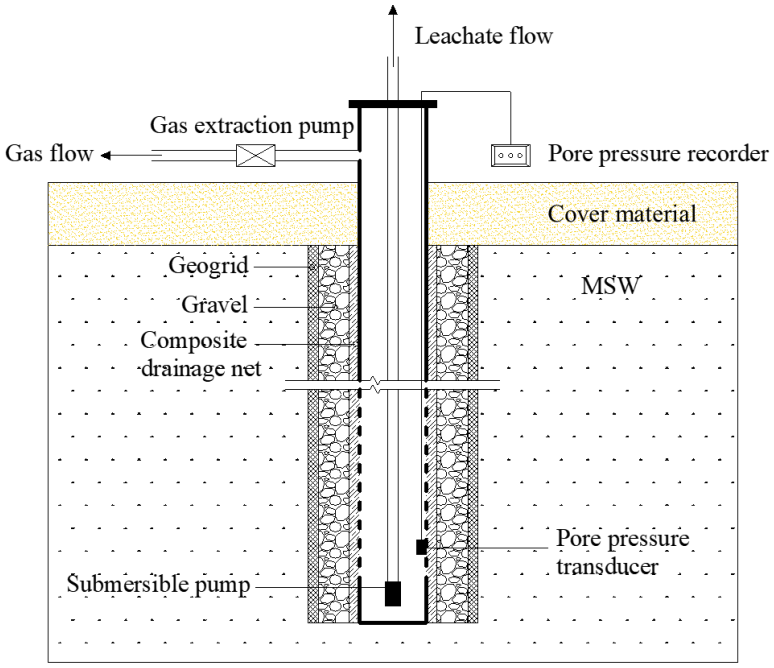


Figure 17. Proposed schematic diagram of a VDW-VP for landfills with high leachate levels.

This study only proposes the conceptual design of the VDW-VP approach to decrease leachate level for landfills, and the practical design needs more specific investigations in the future. For instance, the determination of applied vacuum pressure is supposed to comprehensively consider the well depth, well spacing, and energy consumption. The elevation difference between the submersible pump and pore pressure transducer needs to be carefully studied. In addition, the complexity of the material composition and anisotropy of the MSW may affect the development of entrapped gas zones and drainage efficiency of leachate in MSW. Therefore, intermittent application of vacuum pressure might have great significance and is also of interest for further research.

5. Conclusions

This study aims to preliminarily explore the performance of VDW-VP on leachate drawdown in MSW landfills with high leachate levels. Laboratory model tests were carried out under the conditions with and without gas injection. Vacuum pressure in the range of 0~−9.5 kPa were applied for both of the two conditions. Based on the observations and interpretations of the experiments, the following conclusions can be drawn:

(1) Gas generation and accumulation were successfully simulated by injecting gas into saturated sand. The average pressure of entrapped gas in the sand below the water level was 1.35~4.26 times the atmospheric pressure.

(2) Under the condition with gas injection, the water effluent during the pumping process was continuous before the water level in the vertical well dropped to the bottom (at 35 min~64 min) and became discontinuous after the water level dropped to the bottom. The higher the applied vacuum pressure, the longer the time required for the water level to drop to the bottom. In the stage of continuous water effluent, the water pumping rate decreased with the increase of vacuum pressure. The water level in the sand gradually approached that in the vertical well in the stage of discontinuous water effluent. The above phenomena were also observed in the tests under the condition without gas injection.

(3) Under the condition with gas injection, the water pumping rate and cumulative water pumping volume increased with the increase of vacuum pressure in the stage of discontinuous water effluent, which was different from that observed under the condition without gas injection. The sudden increases and drops of some local pore pressures in the stage of discontinuous water effluent, to some extent, indicated that the increase of vacuum pressure contributed to accelerating the breakthrough and dissipation of the entrapped gas in the sand, thus improving the water pumping capacity.

Author Contributions: Conceptualization, X.X. and G.L.; methodology, D.N.; investigation, C.F.; resources, S.X.; writing—original draft preparation, G.L. and D.N.; writing—review and editing, X.X.; supervision, S.X.; funding acquisition, X.X. All authors have read and agreed to the published version of the manuscript.

Funding: This research was funded by the National Natural Science Foundation of China (No. 52178363) and Natural Science Foundation of Zhejiang Province (No. LY20E080022).

Institutional Review Board Statement: Not applicable.

Informed Consent Statement: Not applicable.

Data Availability Statement: The data presented in this study are available on request from the corresponding author.

Conflicts of Interest: The authors declare no conflict of interest.

References

1. Laner, D.; Crest, M.; Scharff, H.; Morris, J.W.; Barlaz, M.A. A review of approaches for the long-term management of municipal solid waste landfills. *Waste Manag.* **2012**, *32*, 498–512. [CrossRef] [PubMed]
2. Agamuthu, P. Landfilling in developing countries. *Waste Manag. Res.* **2013**, *31*, 1–2. [CrossRef] [PubMed]
3. El-Fadel, M.; Bou-Zeid, E.; Chahine, W.; Alayli, B.J.W.M. Temporal variation of leachate quality from pre-sorted and baled municipal solid waste with high organic and moisture content. *Waste Manag.* **2002**, *22*, 269–282. [CrossRef]
4. Chen, Y.; Wang, Y.; Xie, H. Breakthrough time-based design of landfill composite liners. *Geotext. Geomembr.* **2015**, *43*, 196–206. [CrossRef]
5. Koerner, R.M.; Soong, T.Y. Stability assessment of ten large landfill failures. In *Advances in Transportation and Geoenvironmental Systems Using Geosynthetics*; American Society of Civil Engineers: Reston, VA, USA, 2000; pp. 1–38.
6. Koelsch, F.; Fricke, K.; Mahler, C.; Damanhuri, E. Stability of landfills—The Bandung dumpsite disaster. In Proceedings of the Tenth International Waste Management and Landfill Symposium, Sardinia, Italy, 13–17 October 2005.
7. Zhan, L.; Lan, J.; Li, W.; Chen, Y. Slope Stabilization and Capacity Expansion at Tianziling Landfill in Hangzhou, China. In *The International Congress on Environmental Geotechnics*; Springer: Singapore, 2018; pp. 26–34.
8. Feng, S.J.; Chang, J.Y.; Zhang, X.L.; Shi, H.; Wu, S.J. Stability analysis and control measures of a sanitary landfill with high leachate level. *J. Geotech. Geoenviron. Eng.* **2021**, *147*, 05021009. [CrossRef]
9. Caicedo, B.; Giraldo, E.; Yamin, L.; Soler, N. The landslide of Dona Juana landfill in Bogota. A case study. In Proceedings of the Fourth International Congress on Environmental Geotechnics (4th ICEG), Rio de Janeiro, Brazil, 11–15 August 2002; Volume 11.
10. Merry, S.M.; Kavazanjian, E., Jr.; Fritz, W.U. Reconnaissance of the July 10, 2000, Payatas landfill failure. *J. Perform. Constr. Facil.* **2005**, *19*, 100–107. [CrossRef]
11. Jafari, N.H.; Stark, T.D.; Merry, S. The July 10 2000 Payatas landfill slope failure. *ISSMGE Int. J. Geoengin. Case Hist.* **2013**, *2*, 208–228.

12. Athanasopoulos, G.; Vlachakis, V.; Zekkos, D.; Spiliotopoulos, G. The December 29th 2010 Xerolakka municipal solid waste landfill failure. In Proceedings of the 18th International Conference on Soil Mechanics and Geotechnical Engineering, Paris, France, 2–6 September 2013; pp. 309–312.
13. Zhan, T.L.; Xu, X.B.; Chen, Y.M.; Ma, X.F.; Lan, J.W. Dependence of gas collection efficiency on leachate level at wet municipal solid waste landfills and its improvement methods in China. *J. Geotech. Geoenviron. Eng.* **2015**, *141*, 04015002. [CrossRef]
14. Shu, S.; Li, Y.; Sun, Z.; Shi, J. Effect of gas pressure on municipal solid waste landfill slope stability. *Waste Manag. Res.* **2021**, *40*, 0734242X211001414. [CrossRef]
15. Powrie, W.; Beaven, R.P. Hydraulic properties of household waste and implications for landfills. *Proc. Inst. Civ. Eng.-Geotech. Eng.* **1999**, *137*, 235–237. [CrossRef]
16. Benson, C.H.; Barlaz, M.A.; Lane, D.T.; Rawe, J.M. Practice review of five bioreactor/recirculation landfills. *Waste Manag.* **2007**, *27*, 13–29. [CrossRef] [PubMed]
17. Hu, J.; Wu, X.W.; Ke, H.; Xu, X.B.; Lan, J.W.; Zhan, L.T. Application of electrical resistivity tomography to monitor the dewatering of vertical and horizontal wells in municipal solid waste landfills. *Eng. Geol.* **2019**, *254*, 1–12. [CrossRef]
18. Ma, P.; Ke, H.; Lan, J.; Chen, Y.; He, H. Field measurement of pore pressures and liquid-gas distribution using drilling and ERT in a high food waste content MSW landfill in Guangzhou, China. *Eng. Geol.* **2019**, *250*, 21–33. [CrossRef]
19. Zhan, L.T.; Xu, H.; Chen, Y.M.; Lan, J.W.; Lin, W.A.; Xu, X.B.; He, P.J. Biochemical, hydrological and mechanical behaviors of high food waste content MSW landfill: Liquid-gas interactions observed from a large-scale experiment. *Waste Manag.* **2017**, *68*, 307–318. [CrossRef]
20. Acharya, M.P.; Hendry, M.T.; Martin, C.D. Effect of gas bubbles on pore pressure response in peat beneath a railway embankment. *Can. Geotech. J.* **2016**, *53*, 765–772. [CrossRef]
21. Wang, P.; Han, Y.; Wang, J.; Cai, Y.; Geng, X. Deformation characteristics of soil between prefabricated vertical drains under vacuum preloading. *Geotext. Geomembr.* **2019**, *47*, 798–802. [CrossRef]
22. Li, M.; Chen, Q.; Wen, K.; Nimbalkar, S.; Dai, R. Improved vacuum preloading method combined with sand sandwich structure for consolidation of dredged clay-slurry fill and original marine soft clay. *Int. J. Geomech.* **2021**, *21*, 04021182. [CrossRef]
23. Shan, W.; Chen, H.E.; Yuan, X.; Ma, W.; Li, H. Mechanism of pore water seepage in soil reinforced by step vacuum preloading. *Bull. Eng. Geol. Environ.* **2021**, *80*, 2777–2787. [CrossRef]
24. Wu, Y.; Zhou, R.; Lu, Y.; Zhang, X.; Zhang, H.; Tran, Q.C. Experimental study of PVD-improved dredged soil with vacuum preloading and air pressure. *Geotext. Geomembr.* **2022**, *50*, 668–676. [CrossRef]
25. Hu, J.; Ke, H.; Chen, Y.M.; Zhan, L.T.; Lan, J.W.; Xu, W.J. Improvement of vacuum pressure on pumping performance of vertical wells in municipal solid waste landfills. *Environ. Sci. Pollut. Res.* **2021**, *28*, 41283–41295. [CrossRef]
26. Reddy, C.S.; Mohanty, S.; Shaik, R. Physical, chemical and geotechnical characterization of fly ash, bottom ash and municipal solid waste from Telangana State in India. *Int. J. Geo-Eng.* **2018**, *9*, 1–23. [CrossRef]
27. Nanda, S.; Berruti, F. Municipal solid waste management and landfilling technologies: A review. *Environ. Chem. Lett.* **2021**, *19*, 1433–1456. [CrossRef]
28. Tumuluru, J.S.; Yancey, N.A.; Kane, J.J. Pilot-scale grinding and briquetting studies on variable moisture content municipal solid waste bales—Impact on physical properties, chemical composition, and calorific value. *Waste Manag.* **2021**, *125*, 316–327. [CrossRef] [PubMed]
29. Mohammad, A.; Goli, V.S.N.S.; Barroso, P.M.; Vaverková, M.D.; Singh, D.N. Effect of physico-chemico-biological and operational parameters on composting of organic fraction of municipal solid waste and gaseous products emission. *Environ. Technol. Rev.* **2021**, *10*, 271–294. [CrossRef]
30. Xu, X.B.; Powrie, W.; Zhang, W.J.; Holmes, D.S.; Xu, H.; Beaven, R. Experimental study of the intrinsic permeability of municipal solid waste. *Waste Manag.* **2020**, *102*, 304–311. [CrossRef]
31. Wei, H. Experimental and Numerical Study on Gas Migration in Landfill of Municipal Solid Waste. Ph.D. Dissertation, Zhejiang University, Hangzhou, China, 2007.